DURATION OF MULTIPACTING PROCESSES AND DISCHARGES IN THE LINAC OF IONS

L.D. Lobzov, N.G. Shulika, O.N. Shulika, V.N. Belan*

National Science Center "Kharkov Institute of Physics and Technology", 61108, Kharkov, Ukraine

(Received July 6, 2009)

It is experimentally shown that multipactor processes may be as harmful as other of parasitic discharges and cause significant disturbance in resonator electrodynamic characteristics of an accelerating structure. The disturbance may be evaluated by pulse-shape distortions of a reference rf voltage impulse. Control over duration of multipactor processes within diode gaps of a linac is effected by varying parameters of a self-sustained oscillation system formed by two independent positive feedback circuits (PFC). If two synchronous rf voltage pulses of given amplitude superpose in the accelerating structure, there occurs an impediment to multipactor processes. As this takes place, multipactor processes display minimal duration and do not affect acceleration stability.

PACS: 29.17.+w.

1. INTRODUCTION

Usually the issue of multipactor processes and discharges between electrode surfaces in a linac resonance structure is addressed when the structure undergoes RF excitation. However, to obtain reasonable electrodynamic characteristics at the rated structure frequency it is essential to eliminate all adverse effects caused by secondary electron emission from the electrodes [1-8].

There exists a number of methods for impediment to multipactor discharge, namely, profile modification of accelerating electrodes [9]; the use of special electrode coating [10]; the usage of an auxiliary electrode [11]; application of additional DC voltage [12], etc. It should be remarked that any of the methods abovementioned results in substantial deterioration in electrodynamic parameters of an accelerating structure and makes its design rather complicated.

Integration of a stabilized generator operating at a different frequency into RF power system of an accelerating structure reduces multipactor discharge influence on the structure but makes it difficult to archive required working parameters of the linac [13].

It is also possible to impede multipactor discharge influence using a countercircuit [14]. Although the voltage generated by the countercircuit has the same operating frequency, its phase differs by 180° from the main RF voltage phase. This adds complexity to the generation module of the accelerator. Moreover, to prevent the decrease in total voltage magnitude caused by inverse feedback, additional amplifiers are required. Hence, the RF module becomes rather expensive and complicated in design and operation.

At present, a very effective technique for multipactor discharge suppressing has been proposed at the NSC KIPT [15]. It holds a certain advantage over methods mentioned, namely, there is no need to incorporate modifications either in accelerating structure design or its fabrication and assembling technology. The rated voltage for RF field excitation is a combination of in-phase voltages generated by two independent reactive circuits powered by a common RF power source. As this takes place, operating mode of the source is nominal. The change in any parameter of the positive feedback circuit makes it possible to investigate temporal effects of multipactor discharge and processes on linac electrodynamic characteristics.

The purpose of this paper is to study multipactor discharge and its duration in a single-cavity multigap ion linac.

2. BASICS

Electron motion equation in variable electric field

$$\frac{d^2x}{dt^2} = \frac{e}{m} \cdot E \sin(\omega t + \varphi), \qquad (1)$$

where e is the electron charge, m-electron mass, E-electric field intensity, ω-cyclotron frequency, and φ is the initial phase. Upon integrating (1) under assumption x=d (d being a diode gap length) and $t = T/2$ ($T = 2\pi/\omega$) the solution takes the form [16]:

$$d = \frac{eE}{m\omega^2} \cdot \{\pi \cos\varphi + 2\sin\varphi\}. \qquad (2)$$

Taking into account that $Ed = U$, the expression (2) can be rewritten as

$$eU|(\pi \cos\varphi + 2\sin\varphi)| = m(\omega d)^2. \qquad (3)$$

This formula shows coupling between the voltage, phase and frequency providing an electron could cross the diode gap d in half-period of RF voltage.

*Corresponding author E-mail address: belan@kipt.kharkov.ua

By introducing a dimensionless parameter $\xi = eU/[m(\omega d)^2/2]$ the expression (3) can be rewritten as

$$\xi = \left| \left(\frac{\pi}{2} \cdot \cos\varphi + \sin\varphi \right)^{-1} \right|. \qquad (4)$$

Referring to Fig.1 that presents a plot of dependences (4), the parameter ξ is varying from 0.536 to 0.636 as the initial phase ranges from 0° to 65°. The minimum $\xi_{min} = 0,536$ is observed at $\varphi = 32.5°$. A point that should be mentioned is that discharge stability occurs over the phase range between 0° and 32.5° where the derivate is negative.

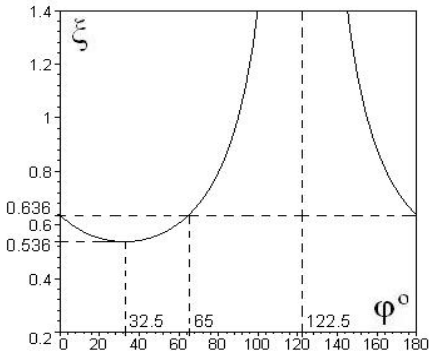

Fig.1. *Phase-dependence of the dimensionless parameter ξ*

3. EXPERIMENTAL PROCEDURE AND RESULTS

Fig.2 depicts a chart for a multigap linac with two independent positive feedback circuits (PFC). Self-oscillations of PFC1 embrace the power source 1 and accelerating structure 3, whereas PFC2 includes the power source 1 along with the feeder 2. It should be pointed out that multipactor processes affect the PFC1 parameters directly.

RF phase and amplitude controllers 4 provide phase and amplitude adjustment in both PFC1 and PFC2. The adder 5 summarizes RF voltages generated by either circuit. Output voltages from PFC1 and PFC2 therewith define resultant fields of the structure.

The accelerating structure 3 used for experiments has been partially described in [17]. It is a periodic resonant H-type facility for proton and deuteron acceleration; it operates at the frequency $f = 100\,MHz$ with a high quality factor $Q_0 \approx 5000$.

Three-step cascade amplification channel serves as a power source. The final cascade is designed to use a pulse triode GI 24A as a basis. The total amplification coefficient for RF power source ranges from 100 to 200 ($K_{amp} \approx 100...200$).

The acceleration channel consists of 17 electrodes (making the number of gaps 16) so placed that π-type axisymmetric electric field is generated. Each electrode (a so called drift tube) is designed as a metallic tube; the tube length and distance between them increase towards the accelerating channel exit. At the beginning of the accelerating channel the distance between the first and second drift tubes makes $1.353\,cm$ and increases up to $1.753\,cm$ between the second and third one while at the end of the channel three last drift tubes are placed $6.120\,cm$ and $6.422\,cm$ apart, respectively.

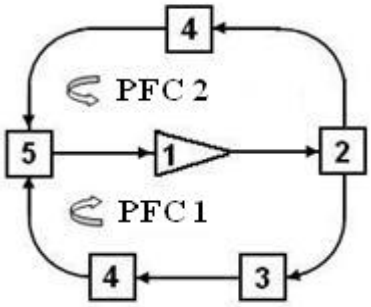

Fig.2. *RF excitation system of single-cavity ion linac: 1 - RF power amplifier, 2 - coaxial feeder, 3 - multigap periodic structure of single-cavity accelerator, 4 - RF phase and amplitude controller, 5 - RF power adder.*
PFC1 - The Contour with the plus feedback of the amplifier channel with RF fields of the accelerating structure, forming its self-oscillatory RF excitation.
PFC2 - The Contour with the plus feedback of the amplifier channel with TEM waves of the coaxial feeder, forming exterior self-excited RF structure

Electric field across annular electrode flanks changes its polarity (i.e. alternates) twice a period. The voltage range over which multipactor processes occur is calculated using the expression (3) and reads $(100...124.6)\,V$ and $(2370...2810)\,V$ across the first and last gap, correspondingly.

It is calculated that accelerating electric field strength across the fist and last gap is $30\,kV/cm$, while this characteristic averaged over all the gaps is $60\,kV/cm$. Hence, the field coefficient for the first and last gap makes 0.5. As this takes place, rated voltage of reference RF pulses is $U_{res} = 8,5\,V$ and $U_{res} = 17\,V$ for proton and deuteron resonant acceleration, respectively.

Coupling cell size for the PFC1 is specified by its amplification coefficient in the range (0.1...0.15) K_{amp} at a small RF field disturbance (less than 1%). Similar small field disturbances over the feeder govern the size for PFC2 coupling element.

The ratio $U_{pfc2} \geq 0,25\,U_{pfc1}$ between PFC1 and PFC2 voltages generated simultaneously is chosen under condition of PFC1 being dominant circuit [17].

Control over operational phase of positive feedback in either circuit makes it possible to establish traveling-wave mode in both the excitation and feeder channels. As this takes place, the amplitude of incident and reflected waves determines conditions for resonant input resistant consistency with feeder wave impedance and the amount of incoming RF power.

As RF field alteration takes place in each gap si-

multaneously, electron current measured at the accelerating structure output reflects the same secondary electron processes that occur across the initial part of the structure. This fact allows us to study secondary electron current by means of Faraday cup intended for accelerated ion diagnostics.

Snapshots on Fig.3 present conjugated RF pulse oscillograms which have been observed for the same resultant accelerating voltage U_{res} (lower curves) and secondary electron current I_{see} (upper curves) emitted from edges of electrode flanks facing the accelerator exit. These diagrams differ from one another other because the second pair of curves has passed through a simple energy analyzer.

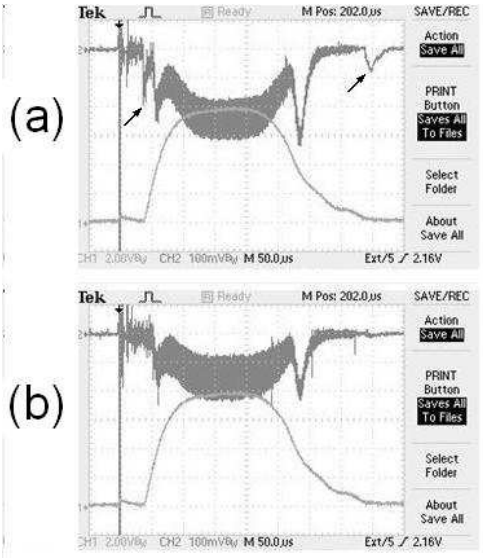

Fig.3. *Conjugated current I_{see} (upper curves) and voltage U_{res} (lower curves) diagrams measured across the penultimate accelerating gap.*

Referring to Fig.3, the current amplitude has several spikes on both the leading and trailing edges (we marked these spikes with arrows). Hence, the multipactor processes are observed not only on the RF voltage impulse front end, but on its rear end as well. It is also obvious that secondary electron current pulses differ in magnitude and length.

As evident from Fig.3(a), low voltage amplitude that corresponds to leading and trailing edges of the pulse is responsible for the secondary electron current spikes. As these spikes appear discretely from impulse main body, it is possible to measure electron energy by means of a thin foil placed before the Faraday cup. The material choice for the foil and its thickness is dictated by specific requirements on absorption of low-energy electrons and partial deceleration of high-energy particles.

Low-energy electrons are fully absorbed by the aluminum target of thickness $5\,\mu m$, as may be seen from Fig.3(b). The decrease in high-energy secondary electron current in the mean portion of pulse and resonance spikes ($I \sim du/dt$, [18]) does not exceed 20%.

It follows from these results that the pattern in which high-frequency voltage amplitude is changing does not affect the initial growth in electron number across the diode gaps of the accelerating structure. In other words, the multipactor processes under attenuating RF fields of low amplitude are governed by the same secondary electrons that are emitted at electric field rise.

It is also possible to investigate the influence of voltage amplitude U_{pfc1} and U_{pfc2} on time evolution of multipactor process if a resonant accelerating structure features the high quality factor Q along with relatively slow RF voltage build-up.

The voltage U_{pfc2} induced by the inductive feedback loop is adjusted by tilting the loop's plane in relation to magnetic field lines of the coaxial feeder. Taking the slope of 0 and 90° degrees as the initial and final position, correspondingly, it is convenient to express the amplitude of induced RF voltage as $U_{pfc2} = U_{pfc2\,nom} \cdot \sin\varphi$ (α is the tilt angle).

If step control of positive feedback coefficient of PFC2 runs in backward direction (from 90° down to 0° degrees), it makes possible to reverse the nature of secondary electron processes. To put it differently, a decrease in voltage amplitude can also cause an avalanche-like increase in secondary electron number across electrodes in the initial part of the accelerating structure.

Phase relation for each oscillation circuit stays at nominal value. The amplitude of modulation pulse generated at the final stage of RF power source defines the value of peak voltage produced by either circuit.

General matching of input resonant structure resistance to wave feeder impedance is governed by minimum of reflected wave amplitude and standing wave coefficient C_{sw} . This allows exerting additional manual control over resonant accelerator characteristics. If the PFC2 coupling element is parallel to magnetic field lines or has a small tilt (of less than 20 degrees), the induced voltage is rather low and stable multipactor discharge is retained. Also a white-bluish glow is observed across two initial accelerating gaps.

As the increasing voltage U_{pfc2} reaches the value $U_{pfc2} = U_{pfc2\,nom} \cdot \sin 20°$ or higher, shape-distorted voltage pulses are beginning to register by the oscilloscope with initial time delay (t_d) and varying amplitude along the pulse length.

Referring to Fig.4a-d, as the voltage U_{pfc2} builds-up in step-like manner, excitation time delay drops from $t_d = 50\,\mu s$ to zero. The pulse frontline clearly exhibits distortions which are typical for a multipactor discharge. It is also evident that the pulse changes its shape and the leading step dwindles in the process [19,20].

At the end of the pulse plateau where decrease rate of resultant voltage amplitude is maximal, the conditions for secondary electron growth are breaking down that, in its turn, leads to multipactor discharge suppression.

With further increase in the PFC2 coupling coefficient along with resultant electric field magnitude growth, the influence of multipactor discharges weakens. This is obvious from the difference in the pulse

leading-edge duration (Fig.4e-g). It is also believed that total distortion of electrodynamic characteristics of the accelerating structure is reduced as well.

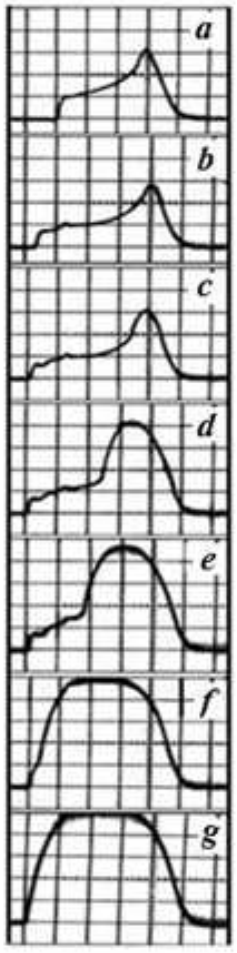

Fig.4. *Presents an oscillogram sequence showing pulse-shape and pulse-duration distortions as the voltage U_{pfc2} increases from zero up to $U_{pfc2nom}$. RF voltage pulses of the accelerator cavity that undergoes multipactor processes influence at rated PFC1 parameters and PFC2 voltage step-controlled: (a)-(f) pulses at fixed tilt angle in the range from 20° up to 70° (every 10°); (g)-RF voltage pulse at tilt angle higher than 70° (up to 90°). Horizontal scale is 50mks per graduation; vertical scale is 2V per division*

As the voltage U_{pfc2} continues to grow and at some moment meets the condition $U_{pfc2} = U_{pfc2\,nom} \cdot \sin 70°$, the multipactor discharge starts to die down till it ceases to exist. Pulse shape in Fig.4(g) provides clear evidence to this process. In this case, increase in energy of electrons bombarding the electrodes results in decrease in secondary emission coefficient.

RF field energy transferred by the electrons determines general electron load and -factor value of the accelerating structure. Complete shape of RF pulse holds no visual distortions of electrodynamic parameters and resonant characteristics of the linac cavity.

The oscillograms provide an experimental verification of high efficiency of this method of multipactor discharges suppression.

4. SUMMARY

Experiments confirm the possibility to control the duration of multipactor discharge in a diode gap of single-cavity accelerating structure by two RF voltages generated by different independent circuits.

The duration of multipactor processes and discharges is defined by generation time of RF voltage induced by the positive feedback circuit with the accelerating structure integrated. Without additional independent reaction circuit ($U_{pfc2} = 0$) multipactor discharge can exist for a long time.

Minimal multipactor discharge duration is determined by resultant RF voltage generated by two independent positive feedback circuits, PFC1 and PFC2, with proper positive feedback coefficients.

Experimental results obtained point to the fact that there exist new possibilities for studies into multipacting phenomenon and development of highly efficient RF structures which are not affected by multipactor discharges.

References

1. V.I. Bobylyov , J.D. Ivanov, A.N. Mishchenko, et al. Protons linear accelerator I-2 // *The Instruments and technique by experiment.* 1967, N5, p.34-39.

2. V.A. Popov. *Positive feedback in RF system linear accelerator LA-20 LHE JINR:* Preprint JINR 9-9192, 1975, Dubna, Russia, 10p.

3. E.V. Gussev, N.A. Hizhnjak, N.G. Shulika, et al. Accelerating H-resonators with high electrodynamics characteristics // *Problems of Atomic Science and Technology. Series "Nuclear Physics Investigations".* 1997, N2,3(29,30), p.187-189.

4. V.L. Auslender, K.N. Chernov, V.G. Cheskidov, et al. Work status of 5MeV, 300kwt electron accelerator // *Thesis of reports of XIX international seminar on accelerators charged particles (Alushta, Crimea), september 12-18, 2005).* Kharkov, Ukraine, 2005, p.31.

5. R.M. Vengrov, V.G. Kuzmichyov, D.A. Liakin. Application of an additional contour of a feedback at excitation of the resonator of the accelerator of heavy ions in an autogeneration mode // *XVII Conference on charged particle accelerators.* Protvino, Russia. 2000, v.1, p.130-133.

6. *Ion linear accelerators. Basic systems*/ Edited by B.P. Murin./ Moscow: "Atomizdat". 1978, v.2, 320p.

7. V.V. Peplov, S.I. Charamentov. System of prompt emergency lockout of power in channels RF supply pouwer // *Basic part LUMF.* Protvino, Russia. 1994, v.1, p.256-259.

8. V.V. Leontev, V.V. Peplov. Acoustic pickup in system of protection against disruptions in a wave-guide feeder of a linear accelerator // *Theses of reports of XX international seminar on accelerators charged particle accelerators. Alushta (Crimea).* Kharkov, Ukraine. 2007, p.90.

9. Aitken D.K. Long-transit-time multipactoring at ultra high frequencies and the effect surface emitting layers // *Proc. I.E.E.1958.* v.105, Suppl.B, N12, p.824-828.

10. V.L. Auslender, et all. Work status of $5\,MeV$, $300\,kW$ Electron Accelerator // *Problems of Atomic Science and Technology. Series "Nuclear Physics Investigations" (47).* 2006, N3, p.3-5.

11. V.G. Veshcherovich, V.K. Sedliarov, V.D. Shemelin. Suppression of the multipactoring discharges in vacuum resonator of storage ring REPB 3 // *Problems of Atomic Science and Technology. Series "Linear accelerators".* 1976, N1(2), p.77-79.

12. B.A. Zager, V.G. Tishin. Resonance RF discharge end possibility its suppression // *JTPH.* 1964, v.34, N2, p.297-306.

13. V.G. Andreev, D.G. Zaidin. Method suppression multipactoring discharges // *Instruments and technique by experiment.* 1971, N3, p.164-165.

14. B.P. Murin. Stabilization and regulation of high frequency fields in ion linear accelerators // *Moscow: "Atomizdat".* 1971, 334p.

15. L.D. Lobzov, N.G. Shulika. Method Suppressing the Multipactoring Discharges // *Problems of Atomic Science and Technology. Ser. "Nuclear Physics Investigations".* 2002, N2(40), p.93-94.

16. L.D. Lobzov, N.G. Shulika, A.P. Tolstoluzhsky. To the theory of electron multipacting in a vacuum cell of linear accelerator // *The Journal of Kharkiv National University. Physikal series "Nuclei, Particles, Fields".* Kharkov, 2005, N657, v.1(26), p.36-46.

17. L.D. Lobzov, P.A. Demchenko, N.G. Shulika, et al. Influence of multipactoring discharges on stability of increase autogenerating accelerating fields in the singl-resonator ion linear accelerator // *The Journal of Kharkiv National University. Physical series " Nuclears, Particles, Fields".* Kharkov, 2003, N585, v.1(21), p.78-84.

18. N.D. Fedorov.*Electron HRF divices and quantum divices.* M: "Atomizdat", 1979, 285p.

19. V.I. Chigin. Physical mechanisms of negative corona pulcation // *Manuscript. Abstract of the thesis for doctor sciences degree of physical-mathematical sciences. O.Ya. Usikov. Radiophysics and Electronics Institute for National Academy of sciences of Ukraine.* Kharkov, 2007, 20p.

20. V.A. Popov. *Excitation of the resonator of linear accelerator LA-20 LHE JINR:* // Preprint JINR 9-9061, 1975, Dubna, Russia, 12p.

ДЛИТЕЛЬНОСТЬ МУЛЬТИПАКТОРНЫХ ПРОЦЕССОВ И РАЗРЯДОВ В ЛИНЕЙНОМ УСКОРИТЕЛЕ ИОНОВ

Л.Д. Лобзов, Н.Г. Шулика, О.Н. Шулика, В.Н. Белан

Экспериментально показано, что мультипакторные процессы могут достигать величин паразитных мультипакторных разрядов и весьма длительно нарушать электродинамические характеристики ускорителя. Нарушение характеристик оценивается по искажению формы контрольного ВЧ-импульса напряжения резонатора. Регулирование длительности мультипакторных процессов и разрядов в ускоряющих зазорах однорезонаторного линейного ускорителя ионов Н-типа, производится изменением параметров результирующих ВЧ-напряжений, возбуждаемых импульсной автоколебательной системой с двумя контурами с независимыми положительными обратными связями. В случае наложения в ускоряющей структуре двух синхронных ВЧ-напряжений номинальных амплитуд, развитие мультипакторных процессов подавляется. При этом длительность процессов минимальна и их влияние на устойчивость характеристик ускорителя отсутствует.

ТРИВАЛІСТЬ МУЛЬТИПАКТОРНИХ ПРОЦЕСІВ І РОЗРЯДІВ У ЛІНІЙНОМУ ПРИСКОРЮВАЧІ ІОНІВ

Л.Д. Лобзов, М.Г. Шулика, О.М. Шулика, В.М. Бєлан

Експериментально показано, що мультипакторні процеси можуть досягати розмірів паразитних мультипакторних розрядів і досить довгостроково порушувати електродинамічні характеристики прискорювача. Порушення характеристик оцінюється по перекручуванню форми контрольного ВЧ-імпульсу напруги резонатора. Регулювання тривалістю мультипакторних процесів і розрядів у прискорюючіх зазорах лінійного прискорювача іонів Н-типу здійснюється зміною параметрів результуючих ВЧ-напруг, збуджених імпульсної автоколивальною системою із двома контурами з незалежними позитивними зворотними зв'язками. У випадку накладення в прискорювальній структурі двох синхронних ВЧ-напруг номінальних амплітуд, розвиток мультипакторних процесів придушується. При цьому тривалість процесів мінімальна і їхній вплив на стійкість характеристик прискорювача відсутній.